protein. On the other hand the fructose-1,6-$P_2$ site was less affected by the proteolytic degradation. This was predicted by the sucrose sedimentation studies which showed that the inactive protein was capable of polymerization in the presence of the sugar bisphosphate in a manner identical with that of the native enzyme.

**Registry No.** ATP, 56-65-5; fructose-6-P, 643-13-0; fructose-1,6-$P_2$, 488-69-7; cyclic AMP, 60-92-4; AMP, 61-19-8; MgATP, 1476-84-2; citrate, 77-92-9; fructose-2,6-$P_2$, 77164-51-3; phosphofructokinase, 9001-80-3; subtilisin, 9014-01-1.

References


Balhorn, R., & Chalkley, R. (1975) *Methods Enzymol. 40E*, 138–144.

Bergstrom, G., Ekman, P., Humble, E., & Engstrom, L. (1978) *Biochim. Biophys. Acta 532*, 259–267.

Botelho, L. H., El-Dorry, H. A., Crivellaro, O., Chu, D. K., Pontremoli, S., & Horecker, B. L. (1977) *Arch. Biochem. Biophys. 184*, 535–545.

Bradford, M. (1976) *Anal. Biochem. 72*, 248–254.

Colombo, G., & Kemp, R. G. (1976) *Biochemistry 15*, 1774–1780.

Colombo, G., Tate, P. W., Girotti, A. W., & Kemp, R. G. (1975) *J. Biol. Chem. 250*, 9404–9412.

Colowick, S. P., & Womack, F. C. (1969) *J. Biol. Chem. 244*, 774–777.

Dautry-Varsat, A., & Cohen, G. N. (1977) *J. Biol. Chem. 252*, 7685–7689.

Dautry-Varsat, A., Cohen, G. N., & Stadtman, E. R. (1979) *J. Biol. Chem. 254*, 3124–3128.

Ellman, G. L. (1959) *Arch. Biochem. Biophys. 82*, 70–78.

Emerk, K., & Frieden, L. (1975) *Arch. Biochem. Biophys. 168*, 210–218.

Gottschalk, M. E., & Kemp, R. G. (1981) *Biochemistry 20*, 2245–2251.

Gottschalk, M. E., Chatterjee, T., Edelstein, I., & Marcus, F. (1982) *J. Biol. Chem. 257*, 8016–8020.

Hummel, J. P., & Dreyer, W. J. (1962) *Biochim. Biophys. Acta 63*, 530–532.

Kemp, R. G. (1969) *Biochemistry 8*, 3162–3168.

Kemp, R. G. (1975) *Methods Enzymol. 42*, 71–77.

Kemp, R. G., & Krebs, E. G. (1967) *Biochemistry 6*, 423–434.

Kemp, R. G., & Forest, P. B. (1968) *Biochemistry 7*, 2596–2603.

Kemp, R. G., Foe, L. G., Latshaw, S. P., Poorman, R. A., & Heinrikson, R. L. (1981) *J. Biol. Chem. 256*, 7282–7286.

Laemmli, U. K. (1970) *Nature (London) 227*, 680–685.

Lindberg, G. M., & Mosbach, K. (1975) *Eur. J. Biochem. 53*, 481–486.

Mathias, M. M., & Kemp, R. G. (1972) *Biochemistry 11*, 578–584.

Ogilvie, J. W. (1980) *Biochim. Biophys. Acta 622*, 277–286.

Paetkau, V., & Lardy, H. A. (1967) *J. Biol. Chem. 242*, 2035–2042.

Parmeggiani, A., Luft, J. H., Love, D. S., & Krebs, E. G. (1966) *J. Biol. Chem. 241*, 4625–4637.

Ramadoss, C. A., Luby, L. J., & Uyeda, K. (1976) *Arch. Biochem. Biophys. 175*, 487–494.

Riquelme, P. T., & Kemp, R. G. (1980) *J. Biol. Chem. 255*, 4367–4371.

Riquelme, P. T., Fox, R. W., & Kemp, R. G. (1978) *Biochem. Biophys. Res. Commun. 81*, 864–870.

Uyeda, K. (1979) *Adv. Enzymol. Relat. Areas Mol. Biol. 48*, 193–244.

Walker, I. D., Harris, J. I., Runswick, M. J., & Hudson, P. (1977) *Eur. J. Biochem. 68*, 255–269.


# Structure and Metabolism of Mammalian Liver Glycogen Monitored by Carbon-13 Nuclear Magnetic Resonance†

Laurel O. Sillerud and Robert G. Shulman*

ABSTRACT: Natural-abundance $^{13}C$ NMR signals from glycogen are observable in situ within the perfused livers of rats. The nuclear magnetic relaxation properties ($T_1$, $T_2$, $\eta + 1$) of glycogen were measured for glycogen in situ and in vitro and were found to be identical. All of the carbon nuclei in glycogen contribute to the high-resolution NMR spectrum, in spite of glycogen's very large molecular weight. The metabolism of glycogen in situ in the perfused rat liver was followed by $^{13}C$ NMR. Stimulation of the fed rat liver by physiological glucagon levels led to rapid glycogenolysis. Perfusion of the liver with [1-$^{13}C$]glucose led to net glycolysis, with concomitant scrambling of the label from $C_1$ to $C_6$ due to triosephosphate isomerase activity.

Carbohydrates ingested in excess of normal metabolic needs are stored initially as glycogen in the mammalian liver. During fasting, glycogen is broken down in order to maintain the blood glucose level near 4.5 mM. The function of liver glycogen is therefore to act as reservoir that can be utilized for glucose homeostasis (Newsholme & Start, 1974).

The structure of glycogen must be compatible with this role in the organism. There is broad agreement that the primary structure of glycogen is adequately explained as a homopolymer of D-glucose with $\alpha(1\rightarrow6)$ links interconnecting the $\alpha(1\rightarrow4)$-linked chains (Goldsmith et al., 1982). Glycogen particles isolated from rat liver (Drochmans, 1962) are large (3–30 nm), which is consistent with the reported molecular weights of $10^7$–$10^9$.

During our continuing program of applying NMR techniques to the study of metabolism in vivo, we discovered that $^{13}C$ NMR signals of glycogen can be obtained from mouse livers perfused with [1,3-$^{13}C$]glycerol (Cohen et al., 1981). We

† From the Department of Molecular Biophysics and Biochemistry, Yale University, New Haven, Connecticut 06511. *Received July 30, 1982.* This work has been supported by the National Science Foundation (PCM-80-21715) and by the National Institutes of Health (5-RO1-AM27121-03).

0006-2960/83/0422-1087$01.50/0 

report here that natural-abundance $^{13}C$ NMR signals from glycogen can be obtained from the livers of rats given ad libitum access to food. In order to establish the utility of these resonances for investigating glycogen metabolism, we have studied their basic $^{13}C$ relaxation properties. In addition, we report the results of experiments which indicate that all the glycogen, either found within the liver or extracted by chemical means, gives rise to high-resolution NMR signals. We discuss how this is possible for a molecule with high molecular weight, since in cellular experiments it is generally only possible to observe rather rapidly tumbling molecules.

Glycogen metabolism is controlled by several means, one of which involves the polypeptide hormone glucagon. Previous attempts to investigate glycogen metabolism have been hampered by the lack of a method of observing liver glycogen in situ. We show here how $^{13}C$ nuclear magnetic resonance spectroscopy can be used to follow glycogen synthesis from [1-$^{13}C$]glucose and glucagon-stimulated degradation in the perfused rat liver.

## Materials and Methods

### *Materials*

*Material Sources.* Sigma Chemical Co. (St. Louis, MO) supplied *Rhizopus* amyloglucosidase, heparin, streptomycin, and rabbit liver glycogen (type V-S). All other reagents were the highest grade available. Glucagon was a gift from Dr. Ron Chance at Eli Lilly (Indianapolis, IN).

### *Methods*

*In Vitro Hydrolysis of Glycogen.* Commercially available rabbit liver glycogen is prepared according to the method of Bueding & Orrell (1964) to preserve the high molecular weight nature of the glycogen particles. Hydrolysis of this material was done by adding 400 mg of glycogen to 2.0 mL of potassium phthalate (50 mM) buffer (pH 4.5) containing 5% $^2H_2O$. A control $^{13}C$ NMR spectrum was taken at $T = 328$ K for 10 min, after which time 1.5 mg of *Rhizopus* amyloglucosidose in 30 $\mu$L of phthalate buffer was added and a series of 10-min accumulations of $^{13}C$ spectra were begun. When glycogens from other preparations were used, these standard conditions were followed, with suitable adjustments made in the amount of enzyme added for the varying amounts of glycogen, to produce approximately 50% hydrolysis during the first hour of the reaction.

*Extraction of Rat Liver Glycogen. (A) Alkaline Extraction.* Livers were isolated from ad libitum fed rats under pentobarbital (50 mg/kg) anesthesia. Glycogen was extracted from the liver by a modification of the method of Somogyi (1934). Briefly, 2 mL of saturated NaOH was added for each g of liver. The liver mixture was heated in a water bath at 100 °C for 2 h, at which time there was complete hepatic dissolution. The red "soap" cake was discarded, and the volume of the clear gelatinous lower phase was doubled with distilled water. The solution was made 33% by volume in ethanol, to precipitate the glycogen, and centrifuged for 10 min. The glycogen pellet was resuspended in distilled water and lyophilized. We found that the liver from an ab lib. fed rat weighed 3.6 ± 0.2% ($n = 20$) of the total body weight. We recovered ~20 mg of glycogen per g of liver, or ~2% of the liver weight.

*(B) Perchloric Acid Extraction.* The liver was freeze-clamped during perfusion (see below) with the aid of a pair of liquid nitrogen cooled aluminum plates (7 × 7 × 0.7 cm) and subsequently ground to a powder in a liquid $N_2$ cooled mortar. All of the following steps were done at 4 °C. The resulting powder was weighed prior to the addition of 4 mL/g of a 7% (v/v) solution of $HClO_4$. This mixture was homogenized for 2 min with a Teflon pestle in a 55-mL glass homogenizer cooled in an ice–salt bath. The homogenate was centrifuged at 10000*g* for 15 min at 4 °C. The pellet was reextracted with ~15 mL of 7% $HClO_4$ and spun as above. The pooled supernatants were neutralized to pH 5.5–6.0 by the dropwise addition of 3 M $CaCO_3$. The precipitated calcium perchlorate was removed by centrifugation at 1000*g* for 10 min, and the resulting supernatant was lyophilized. After dissolution in distilled water, the glycogen was precipitated with 33% ethanol, collected by centrifugation at 4 °C, redissolved in distilled water, and lyophilized prior to usage in further experiments. Our yields with this procedure were identical (2–3% of liver wet weight) with that obtained by using NaOH as mentioned above.

*Glycogen Hydrolysis in Situ.* Under light surgical anesthesia (see above), the portal vein and liver of a rat were exposed through an abdominal incision. Glucagon (5 $\mu$g) in 0.25 mL of Kreb's buffer was injected into the portal vein and allowed to circulate through the liver for ~10 s; the portal vein was then ligated to prevent washout. The liver was quickly excised, placed in a 20-mm thin-wall NMR tube, and surrounded by $^2H_2O$ for a lock solvent. The $^{13}C$ NMR spectrum of this liver was recorded (see below) in 20-min blocks.

*Liver Perfusion.* Liver donors were albino male Charles River rats (70–150 g) previously fed ad libitum. Light surgical anesthesia was employed by using intraperitoneal pentobarbital (see above). The liver was exposed, and with a moderate perfusate flow, a small Lucite cannula was inserted and ligated into the portal vein. The descending aorta and the vena cava were immediately cut, and the pumping rate increased to 4–5 mL $min^{-1}$/(g of liver)$^{-1}$. Livers were then fully excised, rinsed, and placed in a 20-mm thin-wall NMR tube. The tube was sealed with cotton, and perfusate recycling was begun.

The perfusion medium was Kreb's bicarbonate buffer containing 120 mM NaCl, 24 mM $NaHCO_3$, 4.8 mM KCl, 1.2 mM $MgSO_4$, 1.3 mM $CaCl_2$, 1.2 mM $KH_2PO_4$, and occasionally 25 mM 4-morpholinepropanesulfonic acid (Mops). The pH was adjusted to give 7.4 upon equilibration with a 95% $O_2$–5% $CO_2$ gas mixture. The medium was autoclaved before use and then supplemented with streptomycin (100 mg/L) and heparin (1 mg/L).

The perfusion system consisted of a Sage Model 375A peristaltic pump, a Sci-Med Kobolow Model 0200-2A membrane lung, a Corning 125 pH meter employing a Corning 91-15 combination electrode, a Yellow Springs Instruments Model 53 oxygen monitor using a YSI Model 5331 $O_2$ probe, and a Houston Instruments Model B5217-5 dual-channel strip-chart recorder. Teflon tubing (14 awg) was used to connect all components. The tubing and reservoir were autoclaved prior to each experiment. A Lucite bubble trap was used to protect the livers from small bubbles and to house the pH and $O_2$ probes. The total closed system recirculating volume was 85 mL. D-[1-$^{13}C$]Glucose was added to the perfusate to give a final glucose concentration of 30.6 mM. Perfusion was maintained for 4–6 h while the $^{13}C$ spectrum of the liver was monitored to measure the rate of glycogen formation. The livers from ad lib. fed rats synthesized glycogen at a rate of 0.5–1.0 $\mu$mol $g^{-1}$ $min^{-1}$ at 31 °C. Before, and again after the $^{13}C$ spectra of the liver were recorded, $^{31}P$ spectra were taken to monitor the ATP and $P_i$ levels. We found no significant decline in ATP from its initially high (~4.5 mM) level, even after 8 h or more of perfusion. At the end of the experiment, the livers were freeze-clamped, and the glycogen was extracted by either the $HClO_4$ or the NaOH method given

above. No significant difference was found between these methods.

*Nuclear Magnetic Resonance.* Spectra were taken with the aid of a Bruker WH360 wide-bore superconducting spectrometer system. Phosphorus-31 spectra of the perfused livers were taken at 145.8 MHz in a 20-mm probe with a 50-$\mu$s (90°) pulse, a 10-kHz sweep collected in 2048 time domain addresses, and a total time per spectrum of 5.12 min (3000 scans).

Carbon-13 spectra of glycogen were taken at 90.55 MHz in a 10-mm probe with a 70° (27 $\mu$s) pulse repeated every 1.50 s by utilizing a sweep of 6 kHz in 4096 time domain addresses for a total time of 12.5 min (500 scans). Proton noise decoupling (2 W) centered 4.6 ppm downfield from tetramethylsilane ($Me_4Si$) was gated on only during acquisition (0.34 s) to avoid nuclear Overhauser effects. Spin–lattice relaxation times ($T_1$) were measured with the (180°–$\tau$–90°) inversion recovery method and analyzed by using the three-parameter fitting routine from the spectrometer system computer (Aspect 2000) software (DISNMR 810515.1). Nuclear Overhauser enhancements ($\eta$ + 1) were measured from the ratios of the integrated NMR signals obtained during continuous and gated proton decoupling. Spin–spin relaxation times ($T_2$) were measured with the (90°–$\tau$–180°) spin-echo method. Chemical shifts are reported relative to $Me_4Si$ and are referred to $C_{1\beta}$ of D-glucose at 96.71 ppm.

The integrated intensities of the $^{13}$C NMR signals from glycogen and glucose during the hydrolyses were corrected to their exact relative intensities by including adjustments for (a) saturation with respect to $T_1$, (b) pulse angle $\theta < 90°$, and (c) the partial nuclear Overhauser enhancement obtained during the acquisition time. The following equation (Christensen et al., 1974) [where $t$ (seconds) is the total time between pulses, $\theta$ is the pulse angle, $T_1$ is the spin–lattice relaxation time for the particular resonance, $\eta$ + 1 is the nuclear Overhauser enhancement, and $a$ is the acquisition time] was used to compute the true intensity ($M_\infty$) from the measured intensity [$M(t)$]:

$$M(t) = M_\infty \frac{(\sin\theta)(e^{t/T_1} - 1)}{e^{t/T_1} - \cos\theta} + (\eta + 1)(1 - e^{-a/T_1})e^{-t/T_1}$$

The corrections were small for the particular values of $t$ = 1.5 s and $\theta$ = 70° chosen, ranging from 1.000 for glycogen $C_6$ to 1.19 for glucose $C_1$.

$^{13}$C NMR spectra of perfused livers were obtained in 20-mm tubes. Proton decoupling was accomplished by irradiating the sample with 10 W during the acquisition time (0.1024 s) and 2 W during the interpulse delay (0.1024 s). Spectra were typically the average of 5859 free induction decays (total time 20 min) using 4K data points, a 57° (35 $\mu$s) pulse at a repetition rate of 5 s$^{-1}$, and a 20-kHz sweep.

## Results

The proton-decoupled, natural-abundance $^{13}$C NMR spectra of glucose, glycogen, and the liver of an ad lib. fed rat are compared in Figure 1. The assignments of the glucose (Figure 1C and Figure 2) signals follow those of Walker et al. (1976), while the resonances from glycogen (Table I) correlate well with those found for $\alpha(1\rightarrow4)$-glucans (Jennings & Smith, 1973; Colson et al., 1974; Heyraud et al., 1979). It is clear from the spectrum (Figure 1B and 2A) of glycogen that the resonance from $C_1$ is shifted 7.80 ppm downfield from its position in $\alpha$-glucose (92.68 ppm, Table I). This resonance shift is due to the $\alpha(1\rightarrow4)$ linkage of glucose residues to form glycogen. For the same reason, glycogen $C_4$ resonates 7.46 ppm downfield from its position (70.27 ppm) in $\alpha$-glucose.

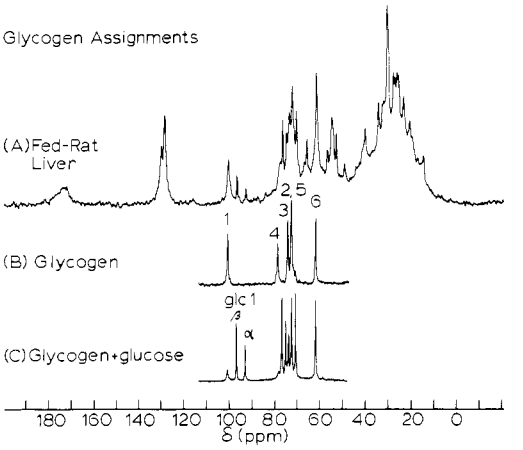


FIGURE 1: Proton-decoupled $^{13}$C natural-abundance NMR spectra from the following: (A) the excised liver (wet weight 12.7 g) from a 374-g rat given ad lib. access to food (10000 scans, 20 min); (B) a solution of rabbit liver glycogen (200 mg/mL) in $^2H_2O$ (500 scans, 20 min); and (C) a mixture of glycogen with $\alpha$-D- and $\beta$-D-glucose (500 scans, 10 min). These spectra show the assignments for the $^{13}$C resonances from glycogen $C_1$–$C_6$ where $C_1$ is the anomeric carbon.

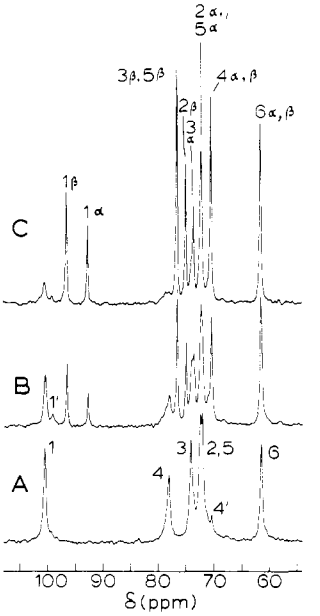


FIGURE 2: Proton-decoupled $^{13}$C natural-abundance NMR spectra of the hydrolysis of glycogen (200 mg/mL) by amyloglucosidase (2 units/mL). Details are given under Methods. (A) Glycogen before enzyme addition; (B) 20 min after enzyme addition; note that some hydrolysis has taken place; (C) 80 min after enzyme addition; the hydrolysis is almost complete.

Table I: $^{13}$C NMR Chemical Shifts (ppm) of Mammalian Liver Glycogen and $\alpha$-D-Glucose at 90.55 MHz and 300 K

| C | (1→4)-glycogen | (1→6)-glycogen | α-D-glucose | $\Delta_{1\rightarrow4}$ [b] | $\Delta_{1\rightarrow6}$ [b] |
|---|---|---|---|---|---|
| 1 | 100.48[a] | 99.22 | 92.68 | 7.80 | 6.54 |
| 2 | 71.96 | 71.96 | 72.06 | 0.04 | −0.10 |
| 3 | 73.96 | 73.54 | 73.39 | 0.57 | 0.15 |
| 4 | 77.73 | 70.03 | 70.27 | 7.46 | −0.24 |
| 5 | 72.21 | 72.21 | 72.06 | 0.15 | 0.15 |
| 6 | 61.37 | 67.88 | 61.37 | 0 | 6.51 |

[a] With respect to $Me_4Si$ at 0.00 ppm. [b] Oligomer minus monomer shielding difference between the glycogen and glucose chemical shifts. A positive $\Delta$ value indicates that the oligomer carbon resonates downfield (i.e., is deshielded) with respect to the monomer.

There is a shoulder at 99.22 ppm on the glycogen $C_1$ resonance that arises from $C_1$ of glucose residues linked $\alpha(1\rightarrow6)$ in

Table II: Carbon-13 Nuclear Magnetic Relaxation Parameters of Rat Liver Glycogen at 300 K and 90.55 MHz

| C | $T_1$ (s) | $T_2$ (ms) | $\Gamma$ (Hz) | $\eta + 1$ | $\tau_c$ (ns) | $r_s$ (nm) |
|---|---|---|---|---|---|---|
| | | | In Vitro | | | |
| 1 | 0.22 ± 0.01 | 31.1 ± 1.4 | 41 | 1.21 ± 0.05 | 4.47 | 1.64 |
| 2 | 0.24 ± 0.03 | | | | 4.79 | 1.68 |
| 3 | 0.22 ± 0.02 | | | | 4.46 | 1.64 |
| 4 | 0.22 ± 0.04 | 32.1 ± 2.1 | 82 | 1.23 ± 0.05 | 4.68 | 1.67 |
| 5 | 0.24 ± 0.05 | | | | 4.90 | 1.69 |
| 6 | 0.11 ± 0.01 | 16.7 ± 1.5 | 43 | 1.18 ± 0.05 | 4.27 | 1.62 |
| | | | In Situ | | | |
| 1 | 0.25 ± 0.01 | 32 ± 6 | 50 | 1.23 ± 0.05 | 5.25 | 1.73 |
| 4 | 0.24 ± 0.03 | 33 ± 6 | 71 | 1.21 | 4.90 | 1.69 |
| 6 | 0.12 ± 0.03 | 17 ± 5 | 51 | 1.17 | 4.90 | 1.69 |

glycogen (Jennings & Smith, 1973). From a comparison of the integral of this signal with that of $C_1$ in the 1→4 links, we can estimate that 7.4% of the glucose units in this sample of liver glycogen were linked $\alpha$(1→6). As a consequence, we also expected to find a signal at 67.88 ppm from $C_6$ involved in $\alpha$(1→6) linkages (Colson et al., 1974); however, no such signal could be detected at the present signal to noise ratio. It is possible that the resonance from $C_6$ in $\alpha$(1→6) linkages is broader than the other resonances as a result of its position at a branch point. Such effects are seen for the resonance from $C_4$ in glycogen (Table II); it is 2 times broader than that for $C_1$. These effects have been observed previously for the branch points of gel-forming $\alpha$-D-glucans (Saito et al., 1976). These data suggest that there is a $\alpha$(1→6) link every 13–14 residues.

*$^{13}C$ Nuclear Magnetic Relaxation in Glycogen.* A comparison of the spin–lattice and spin–spin relaxation times and the nuclear Overhauser enhancements for glycogen is shown in Table II both for measurements performed in vitro and for measurements on these molecules performed in situ in the excised liver from an ad lib. fed rat. The data presented are for resonances from $C_1$–$C_6$ of glycogen in vitro; resonance overlap precluded the independent determination of the relaxation parameters for $C_2$, $C_3$, and $C_5$ in the liver. The spin–lattice relaxation time, $T_1$, of glycogen is 0.23 ± 0.01 s both in vitro and in situ (table II), for $C_1$ through $C_5$, which have one directly bonded proton; it is half that value for $C_6$, which has two protons. No significant variation of the $NT_1$ values of $C_1$–$C_6$ is evident from an examination of the data from glycogen in vitro. The rotational correlation times, $\tau_c$, derived from the $NT_1$ values discussed below, are shown, in Table II, to cluster around 4.60 ns (Doddrell et al., 1972). The fact that the $NT_1$ values and $\tau_c$ values are the same for all of the glycogen carbons implies that the hexopyranoside ring undergoes isotropic rotational reorientation. The motional state of glycogen in the liver must closely resemble that found in vitro, judging from the observation of similar $T_1$ values in both cases.

The other NMR relaxation parameters of glycogen have also been measured. The full width at half-maximum $\Gamma$ (hertz), for the glycogen signals in vitro can be used to determine the effective spin–spin relaxation time, $T_2^* = (\pi\Gamma)^{-1}$. The resonances from $C_1$ and $C_6$ have measured widths of 41 and 43 Hz, respectively, at 300 K, leading to values of $T_2^* \sim 7.6$ ms. A direct measurement of $T_2$ using the Carr–Purcell–Meiboom–Gill $90°-\tau-180°-\tau$ sequence gave values of $NT_2 \sim 30$ ms for both $C_1$ and $C_6$. The difference between $T_2$ and $T_2^*$ likely arises from the contribution of magnetic field inhomogeneities to $T_2^*$. In this regard, it is useful to note that the width of the glucose $C_1$ resonance in Figure 1 is 12 Hz, a value almost 2 orders of magnitude greater than the width of 0.25 Hz predicted from its measured $T_1$ (=$T_2$) of 1.28 ± 0.01 s. When this contribution of field inhomogeneity is subtracted from the widths of the $C_1$ and $C_6$ signals, a value of $T_2^* \sim 11$ ms results, which is closer to the directly measured value of $T_2$, but $T_2^*$ is still less than $T_2$. The possibility exists that a contribution to the width derives from conformationally dependent chemical shift heterogeneity.

The spin–spin relaxation times and the line widths are essentially the same in situ within the liver as they are in vitro. The same is true for the nuclear Overhauser enhancement measured in these two environments (Table II). These facts imply that there is little difference in the motional properties of the glycogen carbon skeleton when the two states are compared. The data are all consistent with isotropic rotational reorientation with a correlation time of ~4.6 ns. The approximate Stokes radius, $r_s$, is related to the correlation time by $r_s^3 = 3kT\tau_c/(4\pi\eta)$ where $k$ is Boltzmann's constant, $T$ is the absolute temperature, and $\eta$ is the viscosity. At a temperature of 300 K and a viscosity of 1 cP, a Stokes radius of 1.66 ± 0.03 nm is calculated. The particles of glycogen in the liver, as seen in the electron microscope, have radii that are somewhat larger (2.5–5.0 nm) (Drochmans, 1962).

*All of the Glycogen Contributes a High-Resolution $^{13}C$ NMR Signal.* The observation of relatively narrow resonances from glycogen at natural abundance in situ within the liver raises questions concerning the nature of these signals. Glycogen is known to consist of chains of oligo($\alpha$-D-glucose), but its exact covalent, three-dimensional structure is still a matter of active investigation. It is clear, however, that particles of hepatic glycogen are large and have molecular weights in the millions. From the sizes and masses of the particles, one can estimate correlation times which predict line widths of $10^3$–$10^4$ Hz; the experimental results (Table II), however, show that the glycogen resonances have relatively long $T_2$ values and narrow lines. One possibility is that only a more mobile fraction of $\alpha$-D-Glc (Glc = glucose) residues contributes to the observed glycogen signal and that there are immobile portions that constitute an "NMR invisible core". Alternatively, our relaxation data suggest that the glycogen structure giving rise to the short correlation times and narrow lines is of mass ~$10^3$–$10^4$ daltons. In this case, a short segment of 10–12 oligo($\alpha$-D-Glc) residues would be expected.

*Glycogen Hydrolysis in Situ.* In order to determine which of these models more closely describes hepatic glycogen, we determined the percentage, $P$, of glycogen that gives rise to a high-resolution $^{13}C$ NMR signal. Our strategy was to compare the NMR signals from glycogen with those from the glucose released during exhaustive hydrolysis. If $P$ <100%, then the NMR signal from the glucose released will be larger than that of the glycogen hydrolyzed. Two separate types of experiments were performed. In the first type, the hydrolysis in situ of glycogen in a liver from an ad lib. fed rat was initiated by means of an injection of glucagon into the portal vein of the rat prior to sacrifice and rapid excision of the liver (see Methods for details). $^{13}C$ spectra of the excised liver were obtained within 20 min. Subsequent 20-min spectra were accumulated and used to monitor the release of glucose from the hydrolyzed glycogen. The results (Figure 3, Table III) show that $P$ = 109 ± 10%, i.e., that the integral of the glycogen $C_1$ signal decreases at the same rate as the increase in the sum of the integral of the glucose $C_{1\alpha}$ and $C_{1\beta}$ signals. In preparing Figure 3, we have used the measured $T_1$'s and nuclear Overhauser enhancements to correct the integrals for partial saturation effects (see Methods). The correction factors were kept to a minimum by using optimal pulse angles according

Table III: Summary of the Results of $^{13}$C NMR Measurements of the Percentage ($P$) of Mammalian Liver Glycogen That Gives Rise to a High-Resolution NMR Signal

| sample | glycogen source | extraction method | hydrolysis method | $P$ (%)[a] |
|---|---|---|---|---|
| 810819 | fed rat liver | none | glucagon, in situ | 109 ± 10 |
| 811111 | rabbit liver | Orrell & Bueding (1964) | amyloglucosidase | 93 ± 7 |
| 820113 | fed rat liver | Somogyi (1934) | amyloglucosidase | 99 ± 6 |
| 820310 | fed rat liver, perfused with [1-$^{13}$C]Glc | perchloric acid | amyloglucosidase | 89 ± 16 |
| 820406 | fed rat liver, perfused with [1-$^{13}$C]Glc | perchloric acid | amyloglucosidase | 99 ± 2 |
| | | | | 98 ± 8[b] |

[a] Mean ± standard deviation. [b] Average of 42 determinations.

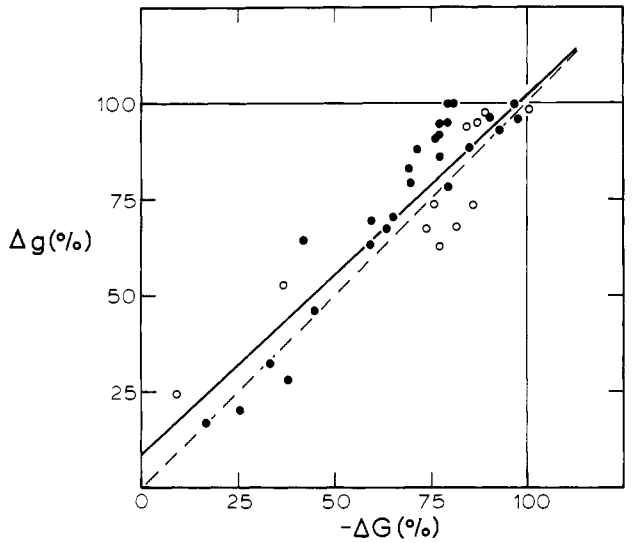


FIGURE 3: Relationship between the decrease in the glycogen $C_1$ $^{13}$C NMR signal, $\Delta G$, and the resulting increase in the sum of the glucose $C_{1\alpha}$ and $C_{1\beta}$ signals, $\Delta g$, during amyloglucosidase-catalyzed glycogen hydrolysis. The results are plotted as the percent of total change in the corrected integrals of signals like those in Figure 2. The solid line is a least-squares fit to the data from all of the individual experiments. The dashed line has a slope of 1.0 for comparison. The open circles refer to hydrolysis in situ by glucagon, while the filled circles refer to the data obtained in vitro.

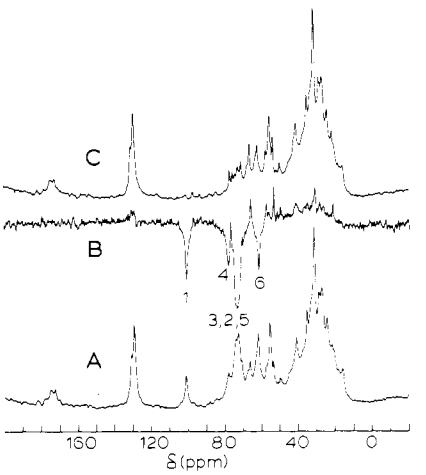


FIGURE 4: Glucagon-stimulated glycogenolysis in the perfused rat liver. (A) Natural-abundance proton-decoupled $^{13}$C NMR spectrum of the liver from an ad lib. fed rat perfused within the bore of the spectrometer magnet; (B) spectrum of twice the difference between (A) and (C) showing the signals from the in situ hydrolyzed glycogen; (C) spectrum of the liver in (A) taken 5 h after treatment with 20 nM glucagon. Note the disappearance of the glycogen resonances.

to $\theta = \cos^{-1}(e^{-\tau/T_1})$ where $\tau$ is the pulse repetition time (Christensen et al., 1974). We also kept the nuclear Overhauser enhancement correction small by gating the decoupler on only during the acquisition.

*Glycogen Hydrolysis in Vitro.* To determine if the commonly used procedures for extracting glycogen from the liver influenced the fraction of NMR-observable glycogen, we examined the changes in the glycogen and glucose $C_1$ $^{13}$C resonances of a number of samples of glycogen prepared by various popular extraction methods. The results (Figure 3, Table III) show that the percentage of NMR-observable glycogen is independent of the source, or extraction, or hydrolysis method employed during the determination. A commercial sample of glycogen, prepared by using the cold water extraction method of Bueding & Orrell (1964), gave $P$ = 93 ± 7%, when hydrolyzed by *Rhizopus* amyloglucosidase. This extraction method was designed to produce a high molecular weight ($M_r \sim 10^7$) glycogen closely resembling that in vivo, so our finding of $P \simeq 100\%$ is consistent with the in situ results presented above.

The NMR-observable fraction of in vitro glycogen isolated in our laboratory by the alkaline extraction method of Somogyi (1934) was found to be 99 ± 6% (Table III). Similar results were obtained from glycogens prepared from a perchloric acid extract of livers perfused with [1-$^{13}$C]Glc. It should be noted that the enzyme, amyloglucosidase, chosen for these hydrolysis experiments cleaves both the $\alpha(1\rightarrow4)$ and $\alpha(1\rightarrow6)$ linkages so that the hydrolyses proceeded to completion (Figure 2).

When all of the results are taken together, we found that $P$ = 98 ± 8%, with no significant difference between hepatic glycogen in situ or extracted glycogen in vitro. Thus, high-resolution signals arise from all of the carbon in glycogen.

*Glucagon-Stimulated Glycogenolysis.* With the assignments and the observability of glycogen in the rat liver at hand, we turned to an examination of the response of these signals to various metabolic perturbations. One of the classical effects, of the hormones that are involved in glucose homeostasis, like glucagon, is to alter the amount of stored glycogen in the liver (Hers, 1976). Figure 4A shows the $^{13}$C NMR spectrum at natural abundance of a perfused liver from an ad lib. fed rat. Signals from monomeric glucose, as observed in the spectrum from an excised liver (Figure 1A), are absent. We have found that the liver from a fed rat generally contains a relatively large amount of glycogen and, when adequately perfused, shows no monomeric glucose signals. Our limit of detection at natural abundance is around 5–10 mM. This is about the physiological concentration of glucose in the blood and liver.

Treatment of this liver, during perfusion, with a physiological concentration of the polypeptide hormone glucagon (20 nM) led to extensive hydrolysis of the endogenous glycogen (Figure 4C) after 5 h. The digital difference spectrum (Figure 4B) shows that little else changed, as far as the other components of the liver are concerned, over 5 h of perfusion. The predominant difference signal arises from the hydrolyzed glycogen. The glucose formed from this glycogen is delivered into the perfusate and diluted by about a factor of 10 with respect to the amount of fluid in the sensitive volume of the probe. The glucose signals are therefore weaker in spectra B or C of Figure 4 than those signals found in the excised liver (Figure 1A) where all of the glucose formed through glycogen

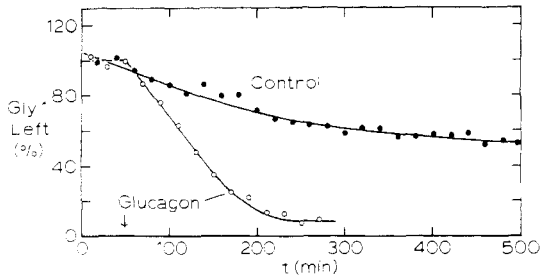


FIGURE 5: Time course of glycogenolysis in situ from the livers of ad lib. fed rats perfused in the spectrometer as in Figure 4. The data are plotted as the percent change in the area of the glycogen $C_1$ signal. The filled circles are the control data taken without the addition of 20 nM glucagon to the perfusate, and the open circles are with the addition.

hydrolysis remains in the NMR coils and is able to contribute to the intensity of the narrow monomer resonances.

One of the problems that may arise during liver perfusion is tissue edema due to hydraulic, osmotic, or metabolic imbalances. Such physical changes in the liver can be monitored by $^{13}C$ NMR by comparing successive spectra with a spectrum taken at the beginning of the perfusion. Swelling displaces a portion of the liver from the NMR coils and leads to a decrease in the ratio of liver tissue to perfusate signals and a marked decrease in the liver background spectrum. It is clear from the lack of difference signals in Figure 4B near 130 ppm, for example, that little or no swelling occurred during this run. We also monitored the size of the liver before and after the perfusion in order to correlate swelling with the difference spectrum. On rare occasions in which swelling did occur, we could easily observe it both visually and spectroscopically. Even though swelling does not seem to markedly affect the metabolic integrity of the liver, it was necessary to be able to monitor it in order to be sure that changes in, for example, the intensities of the triacylglycerol resonances were in response to metabolic rather than physical parameters. It is well-known that the liver can utilize its triacylglycerol stores to provide acetyl coenzyme A (acetyl-CoA) for much of its own energy requirements.

One of the superiorities of the $^{13}C$ NMR method, applied to the study of glycogen metabolism, is the ability to monitor the glycogen content of the liver in situ and in real time on a single liver. The response of the glycogen $C_1$ signal to stimulation by a maximally effective, but still physiological, concentration (20 nM) of glucagon is compared with that for an unstimulated liver in Figure 5. In the control liver, the glycogen signal decays with a half-time, $t_{1/2} > 500$ min; when glucagon was added to the perfusate, this time dropped to 78 min. At the end of this experiment, a $^{13}C$ NMR spectrum of the liver perfusate was obtained, from which a glucose concentration of 21 ± 4 mM was measured. When the total system volume was taken into account, it could be inferred that this liver originally contained at least 353 mg of glycogen. The glucagon-stimulated rate of glycogenolysis was determined to be 0.7 $\mu$mol of Glc $g^{-1}$ $min^{-1}$. These values are well within the ranges determined by other methods.

*Synthesis of Glycogen from Glucose.* During periods of above-normal blood glucose concentration, such as following a carbohydrate-containing meal, the liver no longer needs to hydrolyze glycogen in order to supply glucose to the blood. Instead, the liver is able to switch to glycogenesis in order to store the ingested glucose and to aid in lowering the blood glucose concentration. Perfusion of a fed rat liver with a high concentration (30.6 mM) of glucose (Ross et al., 1967), containing 9.5 mM [1-$^{13}C$, 90%]Glc, resulted in the synthesis

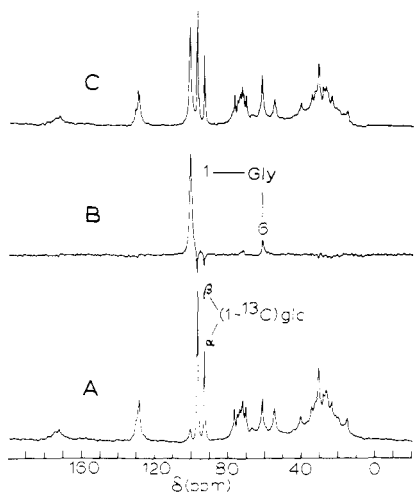


FIGURE 6: Glycogen synthesis from [1-$^{13}C$]Glc in the perfused fed rat liver. (A) Proton-decoupled $^{13}C$ NMR spectrum of the liver 20 min after perfusion with Krebs buffer containing [1-$^{13}C$, 26%]Glc (30.6 mM). (B) Difference spectrum between (A). (C) Spectrum of the liver after 6.2 h of perfusion. Note the 1↔6 scrambling of the label in glycogen, added as $C_1$ of Glc.

of glycogen (Figure 6). The consumption of glucose under these conditions was found to be 0.40 $\mu$mol $g^{-1}$ $min^{-1}$. Several properties of the $^{13}C$ NMR spectra of glucose and glycogen combine to make this approach of particular value in the study of the metabolism of these carbohydrates. The $\alpha$, $\beta$ equilibrium at $C_1$ of glucose results in two resonances from this carbon so that the fate of each anomer can be measured separately. There was no significant difference between the rates of disappearance of the two anomers. The downfield linkage shift to $C_1$ in glycogen with respect to $\alpha$-glucose is large enough so that the signals from the amounts of glycogen and glucose in the liver can be measured simultaneously. For these reasons, the rates of metabolism of both glucose and glycogen can be independently and simultaneously measured.

The difference spectrum (Figure 6B) shows another interesting feature. Not only do we observe the positive glycogen $C_1$ and negative glucose $C_{1\alpha}$ and $C_{1\beta}$ signals but also there is, in addition, a distinct positive signal at 61.5 ppm due to the $^{13}C$ label at glucose $C_6$. The initial glucose was only labeled at $C_1$ with $^{13}C$. The $C_6$ signal comes from glucose that has gone through the first steps of glycolysis to the triosephosphate isomerase step. At that point, $C_1$ and $C_6$ become equivalent, so that the label at $C_1$ appears at $C_6$ when it flows in the gluconeogenic direction back to glucose. We estimate the rate of this futile cycling to be 0.04 $\mu$mol (g of liver)$^{-1}$ $min^{-1}$ or 10% of the rate at which glucose is incorporated into glycogen under the conditions of this experiment (Figure 7).

## Discussion

Previous applications of nuclear magnetic resonance spectroscopy to metabolism have been primarily restricted to studies of small ($M_r$ ~50–1000) molecules, whose size and rapid molecular tumbling result in narrow, high-resolution signals (Hoult et al., 1974; Burt et al., 1976; Hollis et al., 1977; Shulman et al., 1979; Ugurbil et al., 1979). We have recently shown that high-resolution signals from glycogen in situ can be obtained from mouse livers perfused with [1,3-$^{13}C$]glycerol (Cohen et al., 1981) and in vivo from rats fed [1-$^{13}C$]glucose by using topical magnetic resonance (Alger et al., 1981). We have now determined the $^{13}C$ nuclear magnetic relaxation properties, and the amount of glycogen that gives rise to the observed signals, in order to assess the possible utility of these signals for the purpose of monitoring glycogen metabolism.

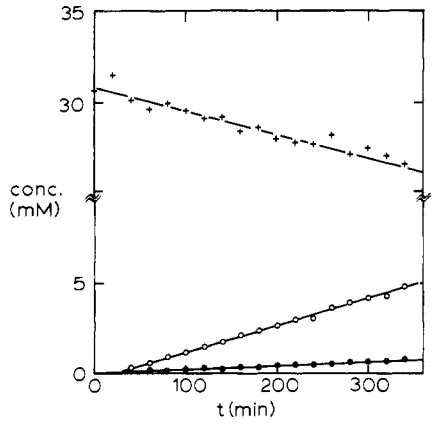


FIGURE 7: Time course of hepatic glycogenesis from [1-$^{13}$C]Glc as described in Figure 6. The filled circles refer to the $^{13}$C NMR signal from $C_1$ of glycogen, the open circles to $C_6$ of glycogen, and the crosses to the sum of Glc $C_{1\alpha}$ plus Glc $C_{1\beta}$.

Our results indicate that glycogen signals are as useful for this purpose as are those from the many small metabolites within the liver cell. The stimulation of glycogen hydrolysis by physiological levels of glucagon was followed in real time, in situ in the perfused liver (Figures 4 and 5), while other experiments demonstrated that the synthesis of glycogen from [1-$^{13}$C]glucose could be followed in a similar fashion (Figures 6 and 7). It is clear that any model of the glycogen particles must be consistent with our $^{13}$C NMR measurements, including the dynamical information derived from the nuclear relaxation data. The fact that all of the glycogen in the liver is observable by means of $^{13}$C NMR implies that the structure of glycogen must allow enough isotropic segmental motion to give a correlation time shorter than that for overall tumbling of what are generally agreed to be large macromolecular particles. Furthermore, the observability of glycogen was found to be independent of the extent of hydrolysis. The cleavage of glucose residues by enzymes in situ or in vitro progresses from the periphery to the center of the particles; thus, our results rule out the existence of a core of glycogen that does not give rise to narrow NMR signals. The motional characteristics of glycogen are uniform throughout the particle, suggesting that the structure does not vary with distance from the particle center. The correlation time (Table II) derived from the $^{13}$C NMR relaxation data can be used to estimate a Stokes radius ($r_s$ = 1.66 ± 0.03 nm) that is smaller than that measured from electron micrographs. This suggests that we are monitoring a substructure smaller than the overall glycogen particle.

All these observations are consistent with a model of glycogen proposed recently by Goldsmith et al. (1982) based on X-ray diffraction data obtained from maltoheptaose bound to phosphorylase. Their model describes the structure of glycogen as composed of short (11–14 residues) helical $\alpha$-(1→4)-glucose oligomers. These are linked $\alpha$(1→6) at the first residue to a prior segment closer to the center of the particle and possess two subsequent segments linked $\alpha$(1→6) to them. A 14-mer of glucose has a mass of 2500 daltons, which is certainly consistent with the estimated size of the glycogen substructure whose relaxation behavior dominates our measurements. The model of Goldsmith et al. (1982) also has the interesting feature that the packing density of helical segments decreases as the center is approached but the structure is otherwise uniform in the sense that it is made up of identical repeating helical segments. The motion of all of these segments must be the same in order to be consistent with our data (Figure 2) showing that all the glycogen has motional characteristics enabling it to give rise to a high-resolution NMR signal independent of the particle size. The structure also may be loosely packed in order to allow the enzymes phosphorylase and glycogen synthetase to work up and down the peripheral segments.

It is significant that, as far as $^{13}$C NMR is concerned, there is no measurable difference between glycogen's structure in situ within the liver cell and as extracted by chemical methods. The milder methods of extraction, such as the cold water method of Orrell & Bueding (1964), have been shown by sedimentation measurements to yield high molecular weight ($\sim 10^7$–$10^8$) particles. These likely represent intact structures present within the cell. The harsher methods utilizing hot KOH (Somogyi, 1934) and perchloric acid necessarily degrade glycogen into smaller ($M_r$ $\sim 10^5$–$10^6$) particles. We believe that our data are derived primarily from smaller substructures in either case: we found no difference because the substructures themselves survive the extraction procedures.

Metabolic changes in the level of glycogen in the liver can be followed by $^{13}$C NMR with the confidence that derives from a firm understanding of the origin of the signals. We illustrated several features of both synthesis and degradation of glycogen by $^{13}$C NMR. Perfusion of a liver with [1-$^{13}$C]-glucose led to the synthesis of glycogen, which could be followed by $^{13}$C NMR coupled with difference spectroscopy. In this case, the substrate contained a $^{13}$C label at $C_1$ so that the flow of carbon atoms from $C_1$ of glucose to other sites or molecules could be followed. Futile cycling of glucose (Katz & Rognstad, 1978) down the glycolytic pathway to the level of the triose phosphates and back up to re-form glucose was found (Figures 6 and 7) which resulted in the appearance of $^{13}$C in glycogen $C_6$. The label moved from $C_1$ to $C_6$ at the level of triosephosphate isomerase.

With the results presented here, we have demonstrated not only the observability of glycogen in situ and in vitro, in agreement with our previous results in vivo (Alger et al., 1981), but also we have shown that glycogen metabolism can be monitored continuously, in real time, within the liver. The way is open to extend these observations to other aspects of glycogen metabolism.

## Acknowledgments

We thank Carl W. Westphal, Eric Brody, Gerry Gollin, and Larry Zisman for assistance with the experiments.

**Registry No.** Glycogen, 9005-79-2; $\beta$-D-glucose, 28905-12-6; $\alpha$-D-glucose, 26655-34-5; glucagon, 9007-92-5.

## References

Alger, J. R., Sillerud, L. O., Behar, K. L., Gillies, R. J., Shulman, R. G., Gordon, R. E., Shaw, D., & Hanley, P. E. (1981) *Science (Washington, D.C.) 241*, 660–662.

Bueding, E., & Orrell, S. A. (1964) *J. Biol. Chem. 239*, 4018–4020.

Burt, C. T., Glonek, T., & Barany, M. (1976) *J. Biol. Chem. 251*, 2584–2591.

Christensen, K. A., Grant, D. M., Schulman, E. M., & Walling, C. (1974) *J. Phys. Chem. 78*, 1971–1977.

Cohen, S. M., Rognstad, R., Shulman, R. G., & Katz, J. (1981) *J. Biol. Chem. 256*, 3428.

Colson, P., Jennings, H. J., & Smith, I. C. P. (1974) *J. Am. Chem. Soc. 96*, 8081–8087.

Doddrell, D., Glushko, V., & Allerhand, A. (1972) *J. Chem. Phys. 56*, 3683–3689.

Drochmans, P. (1962) *J. Ultrastruct. Res. 6*, 141–163.

Goldsmith, E., Sprang, S., & Fletterick, R. (1982) *J. Mol. Biol. 156*, 411–427.

Hers, H. G. (1976) *Annu. Rev. Biochem. 45*, 167-189.
Heyraud, A., Rinaudo, M., Vignon, M., & Vincendon, M. (1979) *Biopolymers 18*, 167-185.
Hollis, D. P., Nunnally, R. L., Jacobus, W. E., & Taylor, G. J., IV (1977) *Biochem. Biophys. Res. Commun. 75*, 1086-1091.
Hoult, D. I., Busby, S. J. W., Gadian, D. G., Radda, G. K., Richards, R. E., & Seeley, P. J. (1974) *Nature (London) 252*, 285-287.
Jennings, H. J., & Smith, I. C. P. (1973) *J. Am. Chem. Soc. 95*, 606-608.
Katz, J., & Rognstad, R. (1978) *Trends Biochem. Sci. (Pers. Ed.) 3*, 171-174.
Newsholme, E. A., & Start, C. (1974) *Regulation of Glycogen Metabolism*, Chapter 4, pp 146-194, Wiley, New York.
Orrell, S. A., & Bueding, E. (1964) *J. Biol. Chem. 239*, 4021-4026.
Ross, B. D., Hems, R., Freedland, R. A., & Krebs, H. A. (1967) *Biochem. J. 105*, 869-875.
Saito, H., Ohki, T., Yoshioka, Y., & Fukuoka, F. (1976) *FEBS Lett. 68*, 15-18.
Shulman, R. G., Brown, T. R., Ugurbil, K., Ogawa, S., Cohen, S. M., & den Hollander, J. A. (1979) *Science (Washington, D.C.) 205*, 160-166.
Somogyi, M. (1934) *J. Biol. Chem. 104*, 245-253.
Ugurbil, K., Shulman, R. G., & Brown, T. R. (1979) in *Biological Applications of Magnetic Resonance* (Shulman, R. G., Ed.) pp 538-589, Academic Press, New York.
Walker, T. E., London, R. E., Whaley, T. W., Barker, R., & Matwiyoff, N. A. (1976) *J. Am. Chem. Soc. 98*, 5807-5813.

# Mapping of the Two Intrachain Cyclic Nucleotide Binding Sites of Adenosine Cyclic 3′,5′-Phosphate Dependent Protein Kinase I†

Stein O. Døskeland, Dagfinn Øgreid, Roald Ekanger, Priscilla A. Sturm, Jon P. Miller, and Robert H. Suva*

ABSTRACT: A series of cyclic nucleotide analogues were examined for their abilities to inhibit the binding of adenosine cyclic 3′,5′-phosphate (cAMP) to each of the two types of cAMP binding sites (A and B) on type I cAMP-dependent protein kinase (cAKI). Sixty-seven different analogues were examined that either contained substituents in the 1-, 2-, 6- (or $N^6$), and/or 8-positions or that included heterocyclic ring systems other than purine. The two sites were found to be similar in that both bound the syn conformation of cAMP and neither formed hydrogen bonds with the adenine ring of cAMP. Moreover, analogues were found that bound preferentially to either site A or site B. Analogues containing bulky, hydrophobic $N^6$-substituents were the most site A specific; for example, $N^6$-(1-methyl-3-phenyl-*n*-propyl)-cAMP was nearly 80-fold more potent as an inhibitor of cAMP binding to site A than to site B. Site B specificity resulted from the presence of either electron-withdrawing substituents in the 2-position or electron-donating substituents in the 8-position; for example, 2-chloro-cAMP and 8-amino-cAMP were approximately 10- and 20-fold, respectively, more potent as inhibitors of cAMP binding to site B than to site A.

The cAMP-dependent protein kinases exist in two isozyme forms: cAKI[1] and cAKII (Corbin et al., 1975). The two isozymes have virtually identical catalytic subunits but dissimilar regulatory subunits (Hofmann et al., 1975). In the absence of cAMP, both isozymes exist as inactive tetramers made up of two catalytic and two regulatory subunits (Hofmann et al., 1975; Rubin & Rosen, 1975). The binding of four molecules of cAMP to the regulatory subunit dimer results in the release of two active catalytic subunit monomers (Corbin et al., 1978).

For both isozymes, the two intrachain binding sites on the regulatory subunit monomers have been shown to be nonidentical based on the rate of [$^3$H]cAMP exchange (Døskeland, 1978; Rannels & Corbin, 1980) and the rate of association with [$^3$H]cAMP (Øgreid & Døskeland, 1981a). In qualitative studies, derivatives of cAMP containing 2- or 8-substituents preferentially inhibited binding to the slowly exchanging B site, whereas the rapidly exchanging A site interacted preferentially with 6-substituted cyclic nucleotide derivatives (Corbin et al., 1982).[2] No studies quantitating the relative affinities of cAMP analogues for sites A and B have appeared.

Site B specific derivatives stimulate the binding of [$^3$H]-cIMP to site A of the holoenzyme, suggesting that interactions between the two sites take place during cAMP activation of the protein kinases (Rannels & Corbin, 1981). Kinetic data have led to the suggestion that binding of cAMP to site B allows the subsequent binding of cAMP to site A (Døskeland & Øgreid, 1981; Øgreid & Døskeland, 1981b). An important, unanswered mechanistic question is whether activation requires binding to only one site or to both sites.

In the present work on cAKI, the $K_I$ values for sites A and B have been determined for a series of cyclic nucleotide derivatives. These data have allowed us to begin mapping the

† From the Cell Biology Research Group, Preclinical Institutes, Årstadveien 19, N-5000 Bergen, Norway (S.O.D., D.Ø., and R.E.), and The Life Sciences Division, SRI International, Menlo Park, California 94025 (P.A.S., J.P.M., and R.H.S.). *Received September 15, 1982.* This work was supported in part by grants from The Nordic Insulin Foundation and The Norwegian Research Council for Sciences and the Humanities (NAVF) (S.O.D.) and in part by U.S. Public Health Service Grant GM25697 from the National Institute of General Medical Sciences (J.P.M.).

[1] Abbreviations: cAKI, cAMP-dependent protein kinase, isozyme form I; cAKII, cAMP-dependent protein kinase, isozyme form II; RI, the regulatory moiety of cAKI; RII, the regulatory moiety of cAKII; C, the catalytic subunit of cAKI or cAKII; Hepes, 4-(2-hydroxyethyl)-1-piperazineethanesulfonic acid; $K_D$, the apparent equilibrium dissociation constant for the interaction between [$^3$H]cAMP and RI; $K_I$, the apparent equilibrium inhibition constant.

[2] In the papers by Rannels & Corbin (1980) and Corbin et al. (1982), the site (A) showing rapid exchange of bound [$^3$H]cAMP is termed site 2, and the site (B) showing slower exchange is termed site 1.

0006-2960/83/0422-1094$01.50/0 